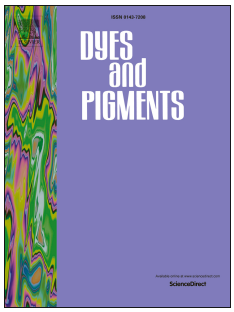

Excited State Relaxation in Cationic Pentamethine Cyanines Studied by Time-Resolved Spectroscopy

Yu.P. Piryatinski, A.B. Verbitsky, A. Dmytruk, M.B. Malynovskyi, P.M. Lutsyk, A.G. Rozhin, O.D. Kachkovsky, Ya.O. Prostota, V.V. Kurdyukov

PII: S0143-7208(21)00405-8

DOI: https://doi.org/10.1016/j.dyepig.2021.109539

Reference: DYPI 109539

To appear in: *Dyes and Pigments*

Received Date: 14 April 2021

Revised Date: 2 June 2021

Accepted Date: 3 June 2021

Please cite this article as: Piryatinski YP, Verbitsky AB, Dmytruk A, Malynovskyi MB, Lutsyk PM, Rozhin AG, Kachkovsky OD, Prostota YO, Kurdyukov VV, Excited State Relaxation in Cationic Pentamethine Cyanines Studied by Time-Resolved Spectroscopy, *Dyes and Pigments*, https://doi.org/10.1016/j.dyepig.2021.109539.

Yu.P. Piryatinski: Conceptualization, Methodology, Validation, Formal analysis, Investigation, Writing - Original Draft, Writing - Review & Editing.

A.B. Verbitsky: Conceptualization, Methodology, Writing - Review & Editing.

A. Dmytruk: Investigation, Data Curation.

M.B. Malynovskyi: Investigation, Data Curation.

P.M. Lutsyk: Conceptualization, Methodology, Formal analysis, Writing - Original Draft, Writing - Review & Editing.

A.G. Rozhin: Methodology, Resources.

O.D. Kachkovsky: Conceptualization, Methodology, Validation, Formal analysis, Investigation, Writing - Original Draft, Writing - Review & Editing.

Ya.O. Prostota: Resources, Validation.

V.V. Kurdyukov: Resources, Validation.

polyene structure

localized charge

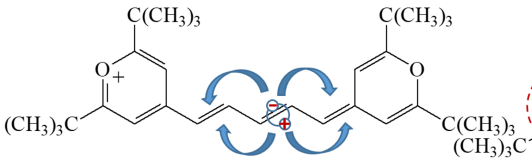

exciton model

polymethine structure

delocalized charge

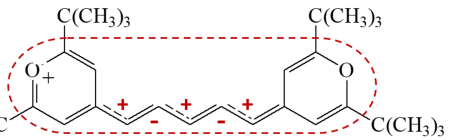

large-radius polaron model

Excited State Relaxation in Cationic Pentamethine Cyanines Studied by Time-Resolved Spectroscopy

Yu.P. Piryatinski[a], A.B. Verbitsky[a], A. Dmytruk[a], M.B. Malynovskyi[a], P.M. Lutsyk[b,*], A.G. Rozhin[b], O.D. Kachkovsky[c], Ya.O. Prostota[c], V.V. Kurdyukov[d]

[a] *Institute of Physics, NASU, Prosp. Nauki 46, 03680 Kyiv, Ukraine*

[b] *School of Engineering and Applied Science, Aston University, Aston Triangle, B4 7ET Birmingham, UK*

[c] *Institute of Bioorganic Chemistry and Petrochemistry, NASU, Murmanska str. 1, 02660 Kyiv, Ukraine*

[d] *Institute of Organic Chemistry, NASU, Murmanska str. 5, 02660 Kyiv, Ukraine*

** Corresponding author email: p.lutsyk@aston.ac.uk; +44 0121 204 4473*

Abstract

In this work, we examined the nature and pathways of electronic excitation relaxation at low temperature in cationic pentamethine pyrylocyanine dye, which in the ground state is characterized by symmetric and non-symmetric localization of cationic charge on the carbon chain between the terminal groups. The carbon chain in such symmetric and non-symmetric charge localizations is close to polymethine and polyene conformations, respectively. The effect of symmetry breaking during the two-way transition polymethine – polyene in the optically excited state on the electronic properties of dyes is considered. Combined quantum-chemical calculations and time-resolved spectral measurements allowed us to characterize the symmetric and non-symmetric structures in the ground and excited states with specific peaks of transitions and lifetimes. The features of the polymethine structure of the dye are attributed to large-radius polaron formation, whereas for the polyene structures the model of excitons formed on the double bonds of the carbon chain can be used to analyze the relaxation pathways. The energy diagram model for relaxation pathways of optically excited electronic states has been proposed. The proposed model can be characteristic for pentamethine cyanine dyes with the symmetric and non-symmetric distribution of cationic charge at the carbon chain between the terminal groups in the ground and excited states.

Keywords

pentamethine pyrylocyanine dye, polymethine and polyene conformations, photoluminescence, time-resolved emission spectra, pump-probe spectroscopy

1. INTRODUCTION

Molecules of polymethine dyes (PMDs) being similar to conjugated oligomers have electronic properties strongly depending on the length and conformational structure of the carbon chain [1-4]. To describe excited states of conjugated neutral oligomers of a polyene structure with alternating single and double carbon bonds, the model of Frenkel excitons is used [5]. According to the model, a neutral quasiparticle of an electron and a hole, exciton, delocalized over the conjugation region is formed via optical excitation. Radiative deactivation of this exciton provides information about the length of the π-conjugation of the carbon chain and its conformation. Furthermore, the electronic properties of conjugated oligomers consisting of a limited number of double and single carbon bonds are attributed to free and self-trapped excitons [6,7]. An additional charge delocalized on the conjugated segment causes a structural rearrangement of the carbon chain. In the optical gap, along with exciton absorption, new allowed states appear, which lead to an additional 'polaron' absorption in the visible and near-infrared spectral range [8]. In the region of localization of the polaron, carbon bonds are aligned, and the excess charge is delocalized along the bonds significantly affecting the optical properties of such molecules [9].

For a cationic (anionic) PMDs, which consists of terminal molecular groups (TGs) and a carbon chain:

$$(TG\text{-}(CH{=}CH)_n\text{-}CH{=}TG)^+ \qquad (1)$$

where *n* is the number of vinylene groups (−CH=CH−), there are two limiting cases in the distribution of excess charge in the molecule. In the first case, the entire charge is localized on one of TGs, the carbon chain can be represented in the form of a polyene structure having excitonic nature of excited states [5]. In the second case, complete delocalization of the entire excess charge along the carbon chain leads to an ideal polymethine structure with aligned carbon bonds (cyanine structure). For such a molecule, large-radius polarons delocalized

along the entire chain are formed in the ground state. Quantum-chemical calculations show that the excess charge forms a polaron delocalized at 6-10 bonds of the chain [10-13]. Such polaron can move along the chain in the ground and excited state of the molecule, change the symmetry of the molecule, and might be captured by defects. The lengthening of the PMDs could cause polaron localization on one of TGs and leads to the so-called "symmetry breaking" in the ground [4] and excited states [14-17]. Depending on the degree of polaron localization, both Frenkel excitons and small-radius polarons could be present in the excited state of the PMD molecule. Such elementary excitations on the carbon chain of a limited length can interact with each other and form charged excitons (trions) [18]. Presented time-resolved spectral studies involving pump-probe methodology has allowed us to elucidate such excitations with direct optical absorption.

Steady-state photoluminescence (PL) spectra of the PMD in solutions at room temperature have a characteristic intense band with a position of the maximum and the width determined by the nature of the solvent [19]. Our group low-temperature studies of time-resolved PL emission spectra (TRES) with picosecond time resolution have shown that several radiation components can be discriminated in these spectra depending on the recording time [15]. In instantaneous TRES, emission bands can be distinguished, the maxima of which are located both on the short-wave side of the absorption band maximum (breaking Kasha's rule [20]) and on the long-wave side. These PL bands are characterized by different delay times with respect to the maximum of the exciting laser pulse and different PL lifetimes. The assumptions about the nature of the emission from PMDs at low temperatures are based on the features of the one-dimensional structure of these dyes: the dependence of the electronic properties in the ground state and excited states on this structure [21], the manifestation of collective electronic excitations [22-24], the dependence of electronic properties on solvation processes that change at low temperatures [25]. The parameters of

quantum-chemical calculations for various molecular geometries [13-15,26,27] provide excellent supplementary insight to such spectral studies.

Previously studied molecule (astraphloxin) as a model for the excited states relaxation [15] has a tendency for aggregation at elevated concentrations [17], which limits its further investigations. Pyrylocyanine (PC) dye having 4-pyrylium terminal rings (Fig. 1a) practically does not aggregate and is highly stable. Moreover, the PC molecule (pentamethine dye, n = 2 in **1**) is longer than astraphloxin (trimethine dye, n = 1 in **1**) and can be distorted much more with symmetry breaking than studied before trimethine astraphloxin. Therefore, the penthamethine PC dye can act as an ideal molecular system for comprehensive analysis of the excited state relaxation by time-resolved spectroscopy and quantum-chemical calculations. The main aim of the current work is a complex investigation of relaxation paths in the optically excited state of the PC dye via time-resolved fluorescence analysis and pump-probe spectroscopy in a wide temporal range of 10^{-8} – 10^{-12} s. Our studies help to establish the nature of the relaxation pathways considering different localization of cationic charge on the carbon chain between the TGs.

2. EXPERIMENTAL SECTION

2.1. Materials. The chemical structure of the PC dye is presented in Fig. 1a. The synthesis of PC dye was described earlier, confirming its structure and constitution by ^{1}H, ^{13}C NMR, IR spectroscopies and elemental analysis [23,28]. The PC dye purity of ≥ 98% was determined by liquid chromatography-mass spectrometry (LC-MS). Steady-state fluorescence studies for PC dye showed the possibility of emission excitation from higher excited states [20]. The PC dye molecule exists in the solvents dissociated into conjugated cation and counter anion (ClO_4^-).

2.2. Absorption and photoluminescence (PL) measurements. UV-Vis absorption spectra were recorded on a Shimadzu UV-3100 spectrophotometer in acetonitrile, dichloromethane, and toluene of spectral grade.

PL measurements were performed in reflection geometry. The steady-state PL spectra were measured using both a USB2000+UV-VIS-ES spectrometer through an optical fiber with a diameter of 600 microns (Ocean Optics B.V.) and by a LifeSpec II spectrofluorometer (Edinburgh Instruments Ltd). To excite the steady-state PL, an MGL-F-532-1.5W laser (CNI Optoelectronics Tech. Co., Ltd.) and an LLS-530 light-emitting diode (Ocean Optics B.V.) were used having a maximum of excitation wavelengths at λ_{EX} = 530 nm, respectively.

Time-resolved PL emission spectra (TRES) and kinetics of PL were studied using the LifeSpec II spectrofluorometer. Furthermore, combining a sequence of PL kinetic curves for different wavelengths of PL emission, a TRES map can be constructed. The TRES map is a spectral contour map plotting PL intensity versus emission wavelength, λ_{EM}, on the X-axis and delay time, *t*, on the Y-axis. To excite time-resolved PL, we used an EPL-405 and EPL-670 picosecond pulsed diode lasers (Edinburgh Instruments Ltd) with λ_{EX} = (405 ± 10) nm and (670 ± 10) nm, respectively. Both lasers have a power of 5 mW and a pulse duration of 54 ps.

To determine the lifetime of excited states of molecules, τ, the technique of time-correlated single-photon counting (TCSPC) is used in the LifeSpec II settings having picosecond temporal resolution of lifetimes. The measured PL intensity $F(t)$ is related to the true decay curve $I(t)$ by the formula (2):

$$F(t) = \int_0^t I\,(t - t')G(t')dt' \tag{2}$$

where $G(t')$ is the instrumental function of the spectrofluorometer, which is the convolution of the Instrument Response Functions (IRF) describing the shape of the excitation pulse. The true decay curve $I(t)$ of PL can be approximated by the expression

$$I(t) = \sum_{i=1}^{n} A_i \exp\left(-\frac{t}{\tau_i}\right) \quad (3)$$

where i is the serial number, τ_i is the lifetime of the excited state, A_i is the weighting coefficient. To measure IRF, a certified colloidal LUDOX solution was used. IRF was considered at the evaluation of τ_i close to the duration of the laser pulse. To calculate τ and to plot the TRES, the F900 software package (Edinburgh Instruments Ltd) was used.

2.3. Pump-probe transient spectroscopy. To study the processes of intramolecular relaxation of electronic excitation, the method of transient absorption spectroscopy (pump-probe) was also used. Transient absorption spectra were measured with the setup of the Femtosecond Laser Complex (NASU) described in detail elsewhere [29,30]. The main pulse of the Ti:sapphire laser (MIRA 900 F; Coherent) at the wavelength of 800 nm, duration of ~150 fs at half-maximum, 1 mJ initial power, 1 kHz repetition frequency was divided into two parts by 1:10. A more intense beam was used to generate the second harmonic of the fundamental frequency of the Ti:sapphire laser, which served as the pump exciting radiation (λ_e = 400 nm, power 10 μJ). A weaker beam after passing through an adjustable delay line was used to generate a supercontinuum serving as probe radiation. The supercontinuum was created by focusing the probe laser beam on a sapphire plate. The studied solutions of the dye in a 1 mm quartz cuvette was placed in the focus of the probe beam. The pump beam was slightly defocused to prevent the formation of bubbles. Part of the supercontinuum was used as a reference beam to calculate absorption. The probe beam after the sample and the reference beam were recorded by an SP-2500i spectrograph (Acton Research). The transient differential absorption spectra were obtained by the formula (4)

$$\Delta D\ (\lambda, t_d) = D\ (\lambda, t_d) - D_0, \quad (4)$$

where $\Delta D\ (\lambda, t_d)$ is defined as the difference in the absorption of a probing supercontinuum by studied solution under the action of a pump beam, $D\ (\lambda, t_d)$, and without the pump beam, D_0. t_d is the delay time between the pump and probe beams. The 3D maps of differential

absorption, $\Delta D\,(\lambda, t_d)$, were plotted showing $\Delta D\,(\lambda, t_d)$ intensity versus wavelength of the probe on the X-axis and delay time, t_d, on the Y-axis.

2.4. Quantum-chemical modeling. The aim of quantum-chemical calculations for PC dye is to study the dependence of electronic structure and electron transitions on the molecular constitution. The GAUSSIAN03 package was used for the modeling [31]. The equilibrium geometry of each dye molecule in the ground state was optimized by the non-empirical DFT/6-31G(d,p)/CAM-B3LYP method. The geometry in the excited state and the electron transition characteristics were calculated by the non-empirical (TD-DFT/6-31G(d,p)/CAM-B3LYP) method. It should be noted that there is no perfect match between the calculated and the experimental data, which is typical for this approach [32,33]. However, obtained values are sufficiently accurate to correctly analyze the nature of electron transitions in studied molecules.

3. RESULTS AND DISCUSSION

3.1. Molecular geometry and electron structure.

The optimization of molecular geometry has shown that the dye molecule is symmetrical and planar in the ground state. Only the six methyl groups (CH_3) are out-of-plane of the conjugated part of the molecule, thus the dye molecule is in all-*trans* conformation. The terminal groups could be treated as a lengthening of the open conjugated chain. The calculations show that optimized C-C bond lengths in the ground state, S_0, are well equalized in the open polymethine chain, which is typical for the PMDs [1,3]. In contrast to the equalized bonds, the atomic charges (q_μ) along the whole chromophore are substantially alternated, which has been confirmed experimentally by ^{13}C NMR spectroscopy [3]. It is known that the excitation of PMDs by a quantum of light is accompanied by a substantial redistribution of the electronic occupancies at atoms and bonds in the dye chromophore [1,3].

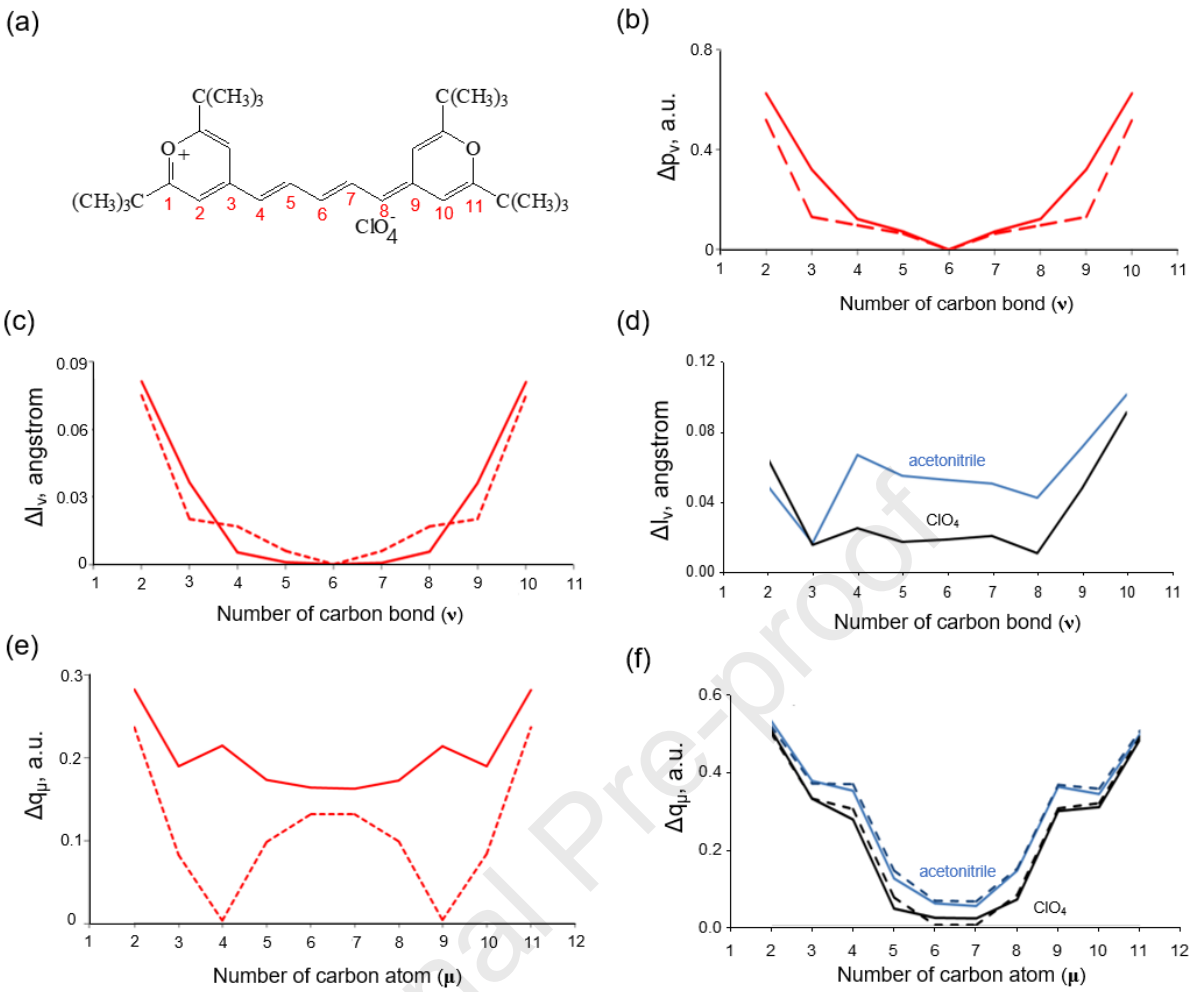

Fig. 1. (a) Chemical structure of the studied PC dye with the enumeration of carbon atoms, μ, in the conjugated chain. (b) Bond order alternations, Δp_ν, (c,d) bond length alternations, Δl_ν, and (e,f) atomic charge alternations, Δq_μ, in the ground (solid line) and excited (dashed line) states. PC dye in the presence of acetonitrile (d,f - blue curves), ClO_4 counter-ion (d,f - black curves), and without counter-ion and no surroundings (b,c,e – red curves).

Therefore, it is beneficial to analyze the charges, q_μ, bond lengths, l_ν, and bond orders, p_ν, using their alternations for the first electron transition:

$$\Delta q_\mu = q_{\mu+1} - q_\mu \quad (5)$$

$$\Delta l_\nu = l_{\nu+1} - l_\nu \quad (6)$$

$$\Delta p_\nu = p_{\nu+1} - p_\nu \quad (7)$$

where μ is an enumeration of carbon atoms (Fig. 1a) and ν are numbers of carbon-carbon bond in the conjugated chain, respectively.

The dependencies of Δq_μ, Δl_ν, and Δp_ν on the atom or bond position are shown in Fig. 1b-e for ground (S_0) and excited (S_1) states. The bond lengths and bond orders are comparatively equalized in the excited state similar to the ground state (Fig. 1b,c). However considerable changes in the carbon-carbon bond lengths upon excitation (< 0.02 Å) remain. Significant atomic charge alternation arises in the excited state (Fig. 1e). Essentially, Δq_μ in the excited state changes its sign in the middle. The function Δq_μ becomes a soliton-like charge wave, which changes its phase upon excitation.

A perturbation of the molecular geometry and charge distribution is possible due to the presence of the counter-ion (ClO_4) or solvent (acetonitrile) molecule (Fig. 1). In Fig. 1d,f, the bond length alternation, Δl_ν, and charge alternation, Δq_μ, are shown under such perturbations, where the ClO^-_4 counter-ion or polar solvent molecules of acetonitrile were located at the distance 3.2 Å from the positively charged oxygen atom in the same plane. The observed perturbations evidence a well-defined symmetry breaking of both bond length and charge distribution in the ground and excited states. Assumingly, the polar solvent could stabilize non-symmetrical conformations of the dye. The perturbations could cause the excess charge (polaron) mobility within the one-dimensional model of the chain [24,34-36]. Thus, the symmetry breaking in the distribution of the excess charge in the PMD can occur in the ground and excited state, and due to symmetry breaking, significant changes in the PL spectra and PL kinetics should be observed.

3.2. Absorption and steady-state fluorescence spectra.

The electron transition characteristics calculated for the ground state geometry correspond to the absorption spectra, whereas the fluorescence spectra are associated with the transitions in the excited state equilibrium geometry [25]. The performed quantum-chemical calculations gave the first electron transition described practically by the single excited configuration: $|\mathrm{HOMO}\rightarrow\mathrm{LUMO}\rangle$ (more details are provided in Supplementary Materials – Table S1, S2).

The relaxation processes in the molecule can lead to a change in its structure, such as valence and torsion angles. A manifestation of such rearrangement is the Stokes shift of the PL spectrum, the change in the quantum yield, and PL lifetimes. To exclude the influence of torsion changes on the electronic structure of the dye in the excited state, the PL spectra were measured at low temperatures (4.2 K), when the solutions are in the solid-state, and the structural changes in the molecules are inhibited due to steric difficulties. In a frozen solution, the distribution of the dyes by symmetry is maintained in its solvate shell. The frozen solvation shell does not track the charge change on the carbon chain under optical excitation. An excited molecule appears in the electric field of an unchanged solvation shell that results in altered distribution of excess charge in the carbon chain and a change of symmetry in the excited state of the molecule.

Absorption spectra of the PC dye were measured experimentally in the highly polar (acetonitrile), weakly polar (dichloromethane) and nonpolar (toluene) solvents and presented in Fig. 2. The steady-state fluorescence spectra for the above solutions are displayed in Fig. 3, whereas the wavelengths of absorption maxima (λ_a^{max}), PL emission maxima (λ_{em}^{max}), and Stokes shifts ($\Delta\nu$) are summarized in Table 1. At 300 K, λ_a^{max} and λ_{em}^{max} are slightly changing at various solvents, whereas the peak positions at low temperature are practically the same for studied solutions. Weak solvatochromism at room temperature (Fig. 2a, 3a) is attributed to electronic and deformation polarizations via an interaction between the solvent shell and charged dye in the ground and excited states. The negligible solvatochromism in

solid solutions (Fig. 2b, 3b), at temperatures below the melting point of the solvent, could be related to the absence of deformation polarization associated with a reorientation of the solvent shell. A more detailed discussion of temperature-dependent solvatochromism is added in Supplementary Materials (Fig. S1-S3).

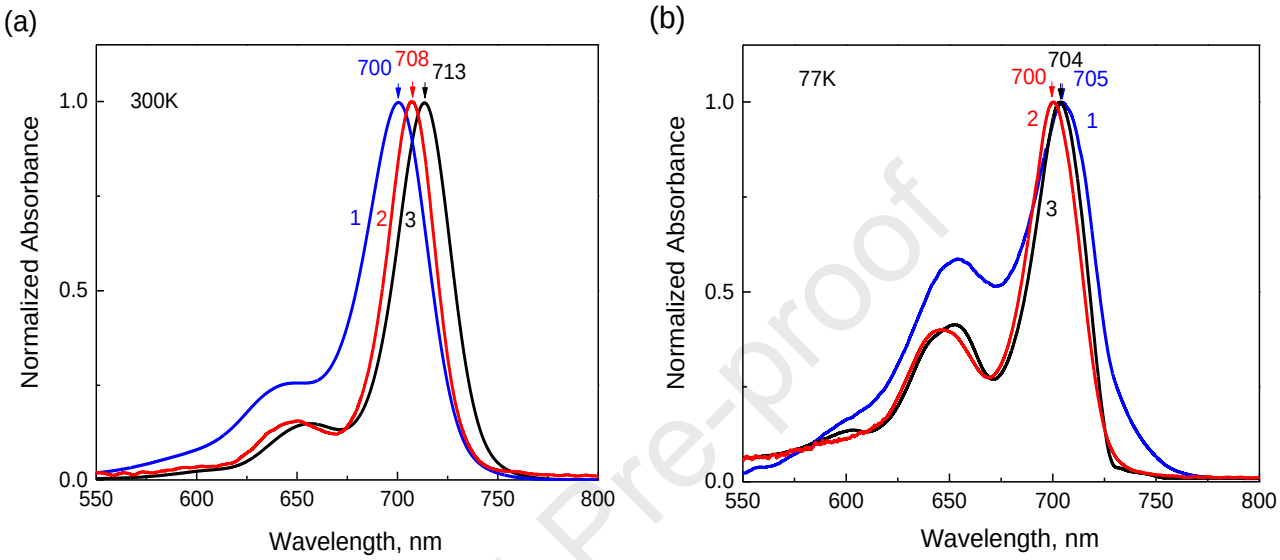

Fig. 2. UV-VIS absorption spectra of the PC dye in acetonitrile (1), toluene (2) and dichloromethane (3) at 300 K (a) and 77 K (b).

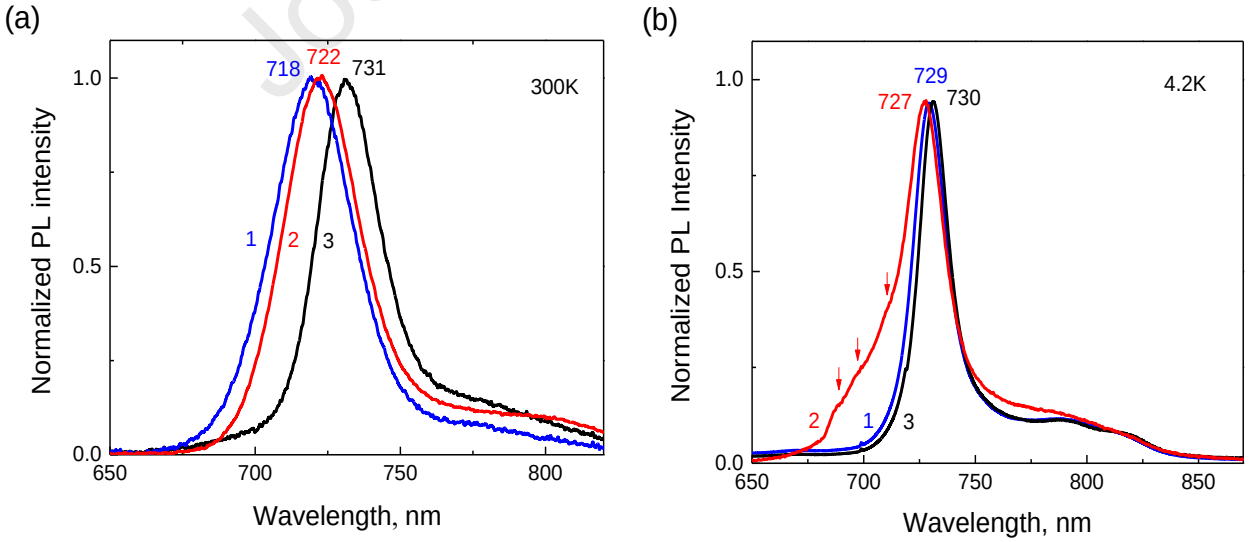

Fig. 3. Steady-state fluorescence spectra of the PC dye in acetonitrile (1), toluene (2) and dichloromethane (3) at 300 K (a) and 4.2 K (b); at λ_{EX} = 530 nm.

The Stokes shift (Δν) featuring redshift of the emission peak (λ_{em}^{max}) relatively to the maximum of absorption (λ_a^{max}) is quite small, which is characteristic to PMDs [37]. Analyzing experimental Stokes shifts in Table 1, Δν slightly changes on solvent polarity and temperature. Besides, the relatively small Stokes shift ($\Delta\nu^{calc}$ = 584 cm^{-1}) was obtained by quantum-chemical calculations (in a vacuum; transition energies were obtained upon the optimized geometry in the ground and excited state). Thus, the calculated value $\Delta\nu^{calc}$ is close to experimental Δν. This fact is in good accordance with the quantum-chemical data showing that the changes in the equilibrium molecular geometry upon the excitation are minimal (Fig. 1c).

Table 1. Absorption maxima (λ_a^{max}), PL emission maxima (λ_{em}^{max}), and Stokes shift (Δν) for the PC dye in acetonitrile, toluene, and dichloromethane.

Solvent	300K			77K (λ_a^{max}); 4.2K (λ_{em}^{max})		
	λ_a^{max}, nm	λ_{em}^{max}, nm	Δν, cm^{-1}	λ_a^{max}, nm	λ_{em}^{max}, nm	Δν, cm^{-1}
acetonitrile	700	720	397	705	729	467
toluene	708	722	274	700	727	530
dichloromethane	713	731	346	704	730	506

3.3. Time-resolved PL decays.

The kinetic decays of PL at a series of emission wavelengths for molecular solutions of the PC dye in acetonitrile and toluene at 300 and 4.2 K are shown in Fig. S4, S5. At low temperatures, the kinetic PL decays for PC molecules in acetonitrile solutions are well described by the three-exponential function:

$$I_{PL}(t) = A_1 \cdot e^{-t/\tau_1} + A_2 \cdot e^{-t/\tau_2} + A_3 \cdot e^{-t/\tau_3} \quad (7)$$

where τ_1, τ_2, and τ_3 are PL lifetimes in the pico- and nanosecond time range and A_n are pre-exponential factors. The PL lifetimes summarized in Table 2 are determined from the exponential fitting of the measured PL decays for studied solutions of the PC dye. The lifetimes are rationalized below considering TRES and pump-probe experiments.

Table 2. Lifetimes of fluorescence (λ_{EX} = 670 nm and different λ_{EM}) for acetonitrile solutions of PC dye at 300 and 4.2 K.

	T, K	λ_{EM}, nm	τ_1, ps	τ_2, ps	τ_3, ps	χ^2	$t_{1/2}$, ps
PC in acetonitrile	300	690	**175**	**363**	–	1.160	**100**
		720	**165**	**371**	–	1.179	**100**
		760	**140**	**381**	–	1.369	**100**
	4.2	710	**70**	**530**	**1690**	1.024	**70**
		720	**160**	**180**	**2200**	1.065	**150**
		730	**140**	**1240**	**2800**	1.019	**265**
		750	**260**	**2260**	**2800**	1.047	**220**
		780	**610**	**2450**	**2480**	1.155	**180**

3.4. Time-resolved emission spectra (TRES) maps and relaxation dynamics.

In contrast to the steady-state PL spectra, the TRES allows one to study the evolution of the spectral characteristics of an excited molecule and to indicate possible ways of its relaxation upon transition to the ground state. Fig. 4 shows the TRES maps for molecular solutions of PC dye as a functional dependence of the PL intensity on two variables – the radiation wavelength (λ_{EM}; Y-axis) and the delay time (t; X-axis). The delay times, t, in recording instantaneous PL spectra were measured relative to the maximum of the laser pulse in the IRF, when t = 0 ns. The cross-section of the maps along the λ_{EM} (Y-axis) gives the

instantaneous PL spectrum for a given *t*, and the cross-section along the delay time (X-axis) corresponds to the PL decay kinetics for a given wavelength. The TRES map for molecular solutions of PC dye at room temperature (Fig. 4a) shows that the shape of the instantaneous PL spectra remains practically unchanged at various *t*. The PL maximum in Fig.4a red-shifts slightly from 718 to 721 nm with *t* change from 0 to 2 ns.

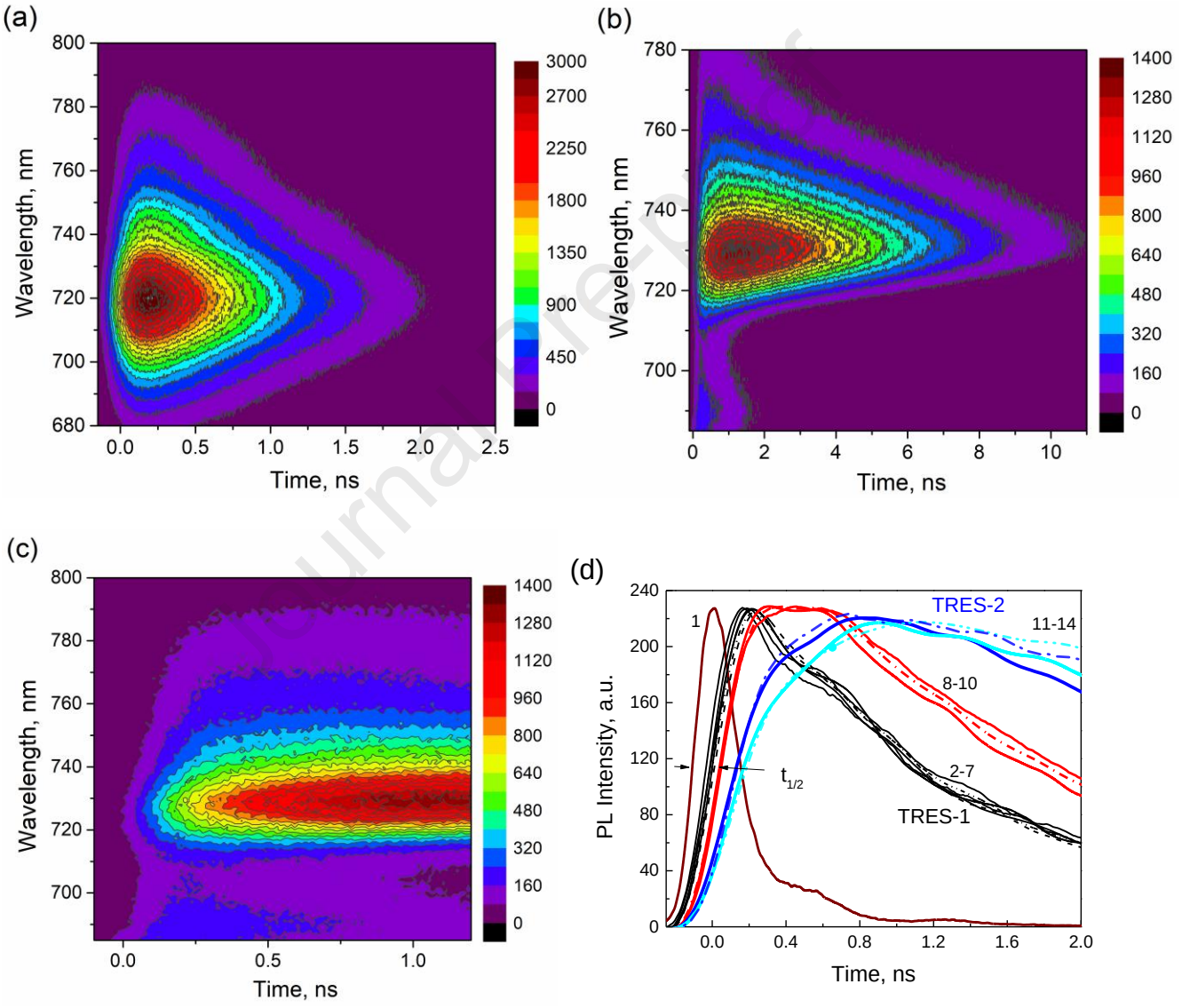

Fig. 4. (a-c) TRES maps at λ_{EX} = 670 nm for PC dye in acetonitrile at (a) 300 and (b,c) 4.2K. (d) PL decays at λ_{EX} = 670 nm for PC dye in acetonitrile at 4.2 K; curve 1 – IRF, curves 2-7:

λ_{EM} = 687-711 nm ($t_{1/2}$ = 70-110 ps), curves 8-10: λ_{EM} = 715-717 nm, ($t_{1/2}$ = 140 ps), curves 11-14: λ_{EM} = 722-745 nm, ($t_{1/2}$ = 230-240 ps).

Low-temperature (4.2 K) TRES map for PC dye in Fig. 4b shows that the fastest changes in the PL spectra occur right after excitation up to 1 ns. At this timescale, one can distinguish a weak PL band in the TRES map peaking at 690 nm. Fig. 4c displays the TRES map with a short timescale for the initial time of *t* up to 1.2 ns. It can be seen from Fig. 4c that PL does not appear immediately after pulsed laser excitation having some time delay. We characterize this time delay with a value of $t_{1/2}$ determined at the half-height of the rising edge of PL kinetic curves relative to the laser pulse peak position. At 4.2 K, the $t_{1/2}$ varies between 70-240 ps depending on the radiation wavelength (Fig. 4c), whereas $t_{1/2}$ = 100 ps from the kinetic curves at room temperature (Fig. 4a). It should be noted that solvation processes could affect the $t_{1/2}$ at room temperature, while low-temperature solid solvent excludes the impact of solvent reorientation.

Analysis of the PL decays in various ranges of the emission in the TRES map (Fig. 4a-c) shows that the kinetics can be divided into two groups (Fig. 4d) characterized by approximately the same $t_{1/2}$ times. The first group encompasses kinetic curves with delay times of $t_{1/2}$ = 70-140 ps (Fig. 4d, curves 2-10), which reflect the processes of PL relaxation in the spectral range of λ_{EM} = 685-720 and 765-800 nm. The first group is denoted as TRES-1. Kinetics with $t_{1/2}$ = 230-240 ps in the range of λ_{EM} = 720-750 nm (Fig. 4d, curves 11-14) fall into the second group, defined as TRES-2. The $t_{1/2}$ in each of the groups are in the same range, however, the lifetimes of PL in each of the groups are different (Table 2).

Fig. 5 shows more detailed TRES for acetonitrile solution of PC dye at 4.2 K in the delay time interval $t < 1$ ns (a) and $t > 1$ ns (b). The fastest changes occur in the spectral

ranges of 680-720 and 750-790 nm, which are attributed to the TRES-1 group characterized by $t_{1/2}$ = 70-140 ps. In the differential PL spectrum (Fig. 5a, curve 11), obtained by subtracting curve 10 (t = 950 ps) from curve 1 (t = 50 ps), several new broad bands are observed having a maximum at 690, 719, and 770 nm. The new bands are not present in the steady-state PL spectra and feature dynamic processes of the TRES-1 group with relatively short $t_{1/2}$. At t varying from 1.05 to 41.05 ns (Fig. 5b), the largest changes in the instantaneous PL spectra occur in the spectral range of 722–760 nm, being attributed to the TRES-2 group. A distinctive new band with a maximum at 748 nm is observed in the PL spectrum at t = 29 ns (curve 6). The average PL lifetime of the emission in the range of this band is approximately 2450-2800 ps (Table 2).

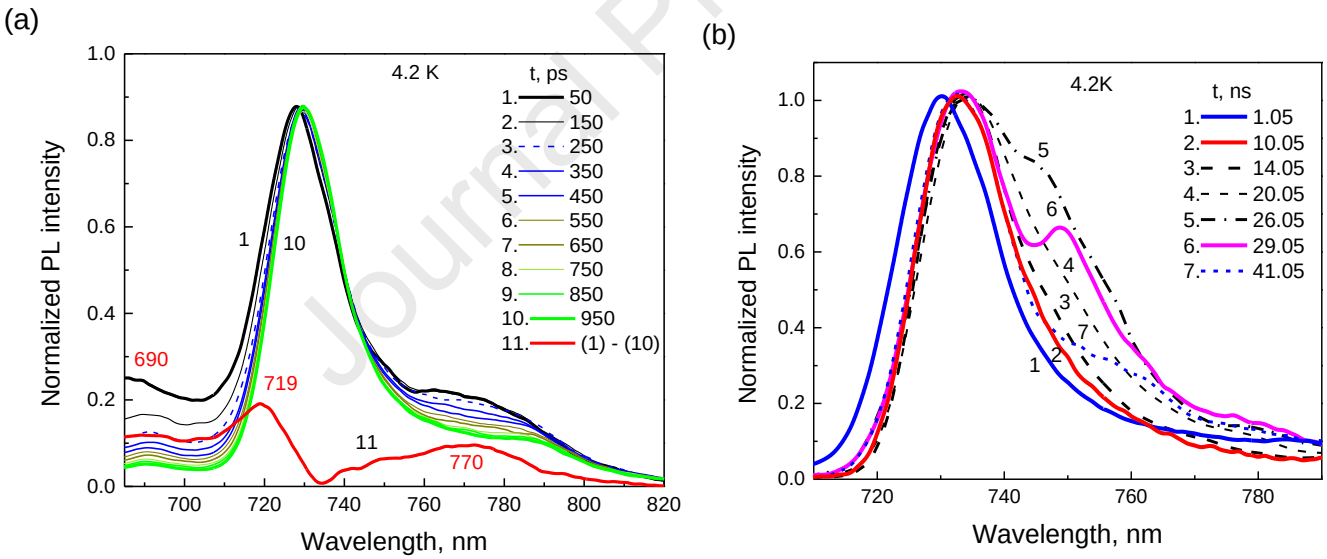

Fig. 5. (a) TRES at λ_{EX} = 670 nm for the PC dye in acetonitrile at 4.2 K in the range of t = 50 - 950 ps with increment of 100 ps (curves 1-10), differential TRES (curve 11) is obtained by subtracting curve 10 (t = 950 ps) from curve 1 (t = 50 ps). (b) TRES at λ_{EX} = 670 nm for the PC dye in acetonitrile at 4.2 K in the range of t = 1.05-41.05 ns; curve 1: t = 1.05 ns, curve 2: t = 10.05 ns, curve 3: t = 14.05 ns, curve 4: t = 20.05 ns, curve 5: t = 26.05 ns, curve 6: t =

29.05 ns, curve 7: t = 41.05 ns. The spectra are normalized to the maximum of the most intense band peaking at approx. 729 nm.

The low-temperature (4.2K) TRES studies of molecular solutions of PC dye in the polar solvent of acetonitrile revealed a PL band with a maximum at 690 nm being in the anti-Stokes spectral region of studied solutions (Fig. 5a). For PC dye solutions in non-polar toluene at low temperatures of 4.2-60K, the PL band peaking at 693 nm can be observed in TRES (Fig. S6). The results can be explained by the fact that, in the ground state, along with the molecules with symmetric charge arrangement in the carbon chain, there are dye molecules with a non-symmetric charge distribution. The anti-Stokes component of PL peaking in the range of 690 nm can be associated with the emission of molecules with a non-symmetric arrangement of charges in the carbon chain in the ground state. Thus, the TRES-1 component in our consideration characterizes the processes of radiative and nonradiative relaxation of electronic excitation for molecules with non-symmetric charge distribution in the ground state. In contrast, the TRES-2 can be associated with relaxation processes in PC molecules with a symmetric distribution of excess charge in the carbon chain in the ground state.

Furthermore, the TRES-1 and TRES-2 bands, which are closely positioned to the maxima of steady-state PL spectra (727-730 nm, Fig. 3b), can be associated with the emission of molecules with a symmetric distribution of charge in the excited state. For TRES-1 at 4.2 K, it relates to the bands at 716 nm (Fig. S6) and 719 nm (Fig 5a) for solutions of the dye in toluene and acetonitrile, respectively. For TRES-2 at 4.2 K, these are intense bands with PL maxima at 729 (Fig. S6) and 730 (Fig 5a) nm for solutions of the dye in toluene and acetonitrile, respectively.

The long-wavelength PL bands can be attributed to the emission of molecules with broken symmetry in the charge distribution in the excited state. For the acetonitrile solution of the dye at 4.2 K, this is the band with a maximum at 748 nm (Fig. 5b). For the toluene solution of PC dye at 4.2 K, no long-wavelength PL band is evidencing no symmetry breaking associated with the transition from the symmetric to the non-symmetric form of the molecule in the excited state.

All PL bands have their vibrational structure, and general vibrational structure in fluorescence bands is complex, especially for low-temperature spectra of steady-state (Fig. 3) and time-resolved PL (Fig. 4-5). The long-wavelength broad bands of PL in the range of 765 – 800 nm could be attributed to such complex vibrational transitions. Thus, studied TRES and PL kinetics indicate the complex electronic structure of the cationic PC dye molecule during its relaxation from the excited to the ground state.

The spectral properties of cationic PMDs are significantly affected by the presence of an excess charge [38,39]. Depending on the length of the carbon chain, solvent polarity, and temperature, the excess charge can be completely (polaron of large radius) or partially (polaron of small radius) delocalized on the carbon chain and have both symmetric and non-symmetric distribution relative to its center. Such changes in the carbon chain lead to changes in the electronic properties of molecules and features in the absorption and PL spectra. PL bands identified in the TRES (Fig. 4-5) cannot energetically belong to the polarons already formed in the carbon chain of the dye in the ground state. Therefore, mobile intramolecular excitations corresponding to the studied PL spectra can be collective involving the formation of charged excitons (trions), formed by molecular excitation (exciton) and polaron [18,40]. The absorption spectra of charged excitons and polarons can be observed by transient absorption spectroscopy (pump-probe) [18,40-42].

3.5. Pump-probe transient spectroscopy.

The differential spectra ΔD (λ, t_d) of transient absorption over time for acetonitrile solutions of the PC dye are presented as 3D maps in Fig. 6. The 3D maps are plotting the intensity of differential absorption, ΔD (λ, t_d), versus wavelength of the probe (X-axis) and delay time, t_d, (Y-axis). In Fig. 6a, the bleaching band in the spectral region of 695-705 nm is characterized by a strong negative signal associated with the depletion of the population of the ground state of the molecules. The amplification region in the range of 710-722 nm have a moderate negative signal (Fig. 6), and most importantly the induced absorption in the spectral range of 765-775 nm has a positive signal (Fig. 6b). Fig. 7 shows the differential absorption spectra ΔD (λ, t_d) for acetonitrile solutions of PC dye in the characteristic spectral regions of the bleaching (curve 1), amplification (curve 2), and induced absorption (curve 3).

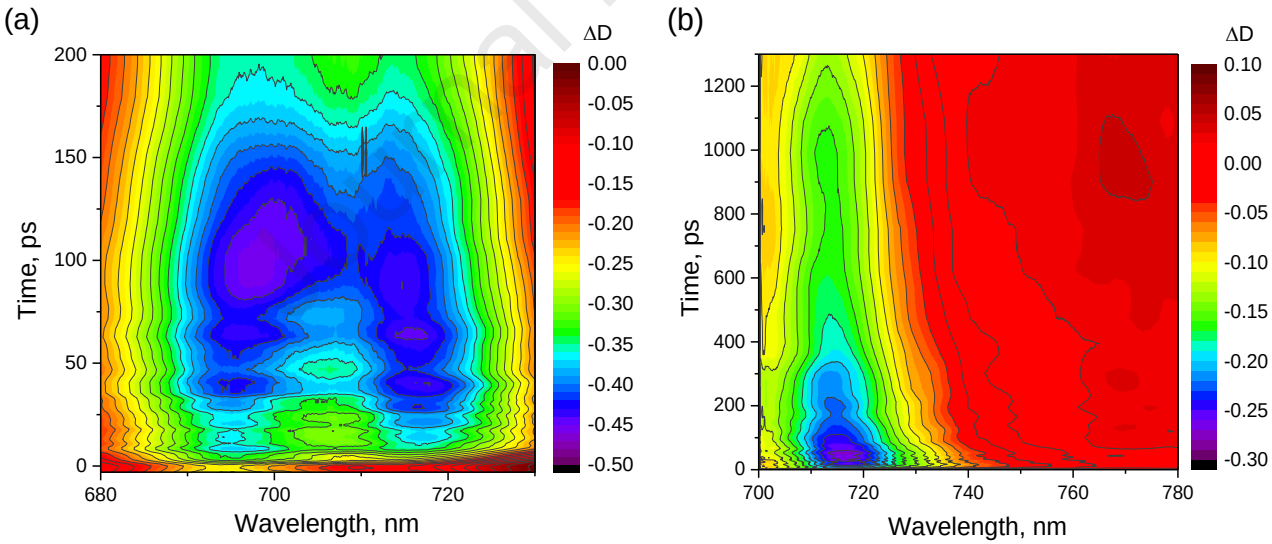

Fig. 6. Maps of transient differential absorption spectra ΔD (λ, t_d) versus wavelength of the probe and delay time for acetonitrile solution of PC dye at 300K.

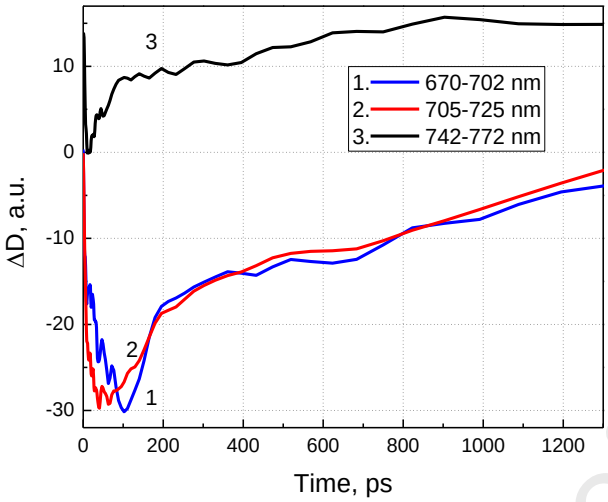

Fig. 7. Kinetics of the differential absorption spectra ΔD (λ, t_d) for acetonitrile solution of PC dye at 300K.

The maps in Fig. 6 and kinetics in Fig. 7 allow us to analyze in detail the temporal and spectral changes of differential absorption. A decaying region just after optical excitation with a characteristic time of t_d = 4-8 ps is observed. Furthermore, the decay reaches a minimum value at t_d = 40-100 ps in the bleaching and amplification ranges. The minimum is followed by two recovery kinetics: one fast in the range of 100-150 ps and another slow recovery ranging approx. 1.2-1.5 ns (Fig. 7, curves 1,2). The induced differential absorption (Fig. 7, curve 3) also has two recovery regions: one fast with a characteristic time of about 70 ps and another slow at approx. 900 ps. The minimum of the bleaching band redshifts from 695 to 699 nm during t_d = 4-100 ps (Fig. 6a) and returns back over the next 100 ps. In the time interval of 4-40 ps, the minimum of the amplification band redshifts from 715 to 717 nm (Fig. 6), and over the next 150 ps, returns to 714 nm. Finally, the induced absorption band at 770 nm reaches its maximum value with a delay time of 800-1100 ps.

The changes in the differential absorption spectra with time are attributed to various structures of the PC molecule in solution — its polymethine and polyene forms. During the

absorption of a quantum of light from pulsed (150 fs) laser excitation, only the electronic state changes in the studied molecule, without alternation of the equilibrium state of the molecule. During this short time, neither the carbon chain nor the solvent shell around the dye molecule has time to change its configuration. The observed initial decay in the range of 4-8 ps can be associated with changes in the electronic subsystem of the PC molecule. The fastest changes in the electronic subsystem of the dye molecule can be attributed to changes in the electron populations of bonds and atoms in the carbon chain, when a polymethine limit structure is established with maximally aligned bonds and alternating in sign charges on carbon atoms. Subsequently, at 40-100 ps, the bond lengths in the carbon chain of the PC molecule equalize to the corresponding populations. This process can be considered as the formation of a large radius polaron and is associated with the establishment of a polymethine structure with maximally aligned bonds and alternating charges on the carbon atoms.

The process of electronic relaxation of studied molecules into the initial form is observed in 100-150 ps, which is characterized in the kinetics of differential absorption by a short-wavelength shift of the bleaching and amplification bands. In addition to the deformation of the carbon chain associated with the alignment of bond lengths, there is a deformation of the solvent. At solvent deformation, the energy of the system decreases, excess energy is absorbed by the solvent, and polarons of small radius might be formed in the chain. Assumingly, the formation of small radius polarons and their interaction with incident radiation corresponds to a wide band of induced absorption with a maximum at 770 nm and t_d = 1000 ps (Fig. 6b), which can be attributed to the formation of charged excitons.

3.6. Model of electronic relaxation pathways in the excited state of PC dye.

The nonradiative and radiative relaxation processes occur in the PC molecules after the Frank-Condon (FC) transition to the excited state, which are reflected in the kinetics and

instantaneous spectra of PL (TRES). The first thing to note is the time delay, $t_{1/2}$, in the PL kinetics after pulsed laser excitation (Fig. 4, Table 2). $t_{1/2}$ can be associated with the processes of the maximum change in the charge density on the carbon chain and aligning the bond lengths in the carbon chain, thus establishing the polymethine state. The time delay $t_{1/2}$ is 70-110 ps for TRES-1, and $t_{1/2}$ = 230-240 ps for TRES-2. Subsequently, due to the symmetry breaking in the distribution of the charge, the carbon chain deforms, and this is leading to the localization of excitation with the formation of a polaron of a small radius. In such a case, the PL band shifts to the long-wavelength side from 725 to 730 nm (Fig 5a). Then due to the symmetry breaking and formation of a small radius polaron, a 748 nm (Fig 5b) band appears on the long-wavelength side of the 730 nm band.

To summarise the relaxation paths of the optically excited states in the studied dye molecule, the energy diagram in Fig. 8 has been proposed. In this diagram, the absorption (long-wavelength band in Fig. 2) refers to the transition of an electron from the ground state E^S_0 to the excited FC state E^+_{FC} of the predominant polymethine structure without changing the equilibrium geometry of the molecule. Following the transition to E^+_{FC}, rapid changes occur in the symmetrical populations of electrons at the atoms and bonds (Fig. 1) with the equilibrium geometry unchanged. This redistribution of electronic populations at atoms and bonds is happening by reducing the energies of the excited state to the state E^S_{R1}. After this, the process of relaxation of molecular excitation to the E^S_{R2} state begins, which is associated with a change in the geometry of the molecule: bond lengths change according to the bond orders in the excited state (Fig. 1b,c). The transition time to this state, taking into account nonradiative processes of establishing electronic populations of bonds and atoms, as well as establishing bond lengths corresponding to an excited state, is $\tau^+_{R1} + \tau^+_{R2}$ = 70-140 ps. The fast recovery of induced absorption (in the range of 100 ps) can characterize $\tau^+_{R1} + \tau^+_{R2}$ on the energy diagram. The radiative transition of an electron from the excited state E^S_{R2} to the

ground state E^S_0 is associated with the PL band at 730 nm and τ^+_2 = 1240 ps (Fig. 8, the TRES-2 group of polymethine state; τ_2 in Table 2).

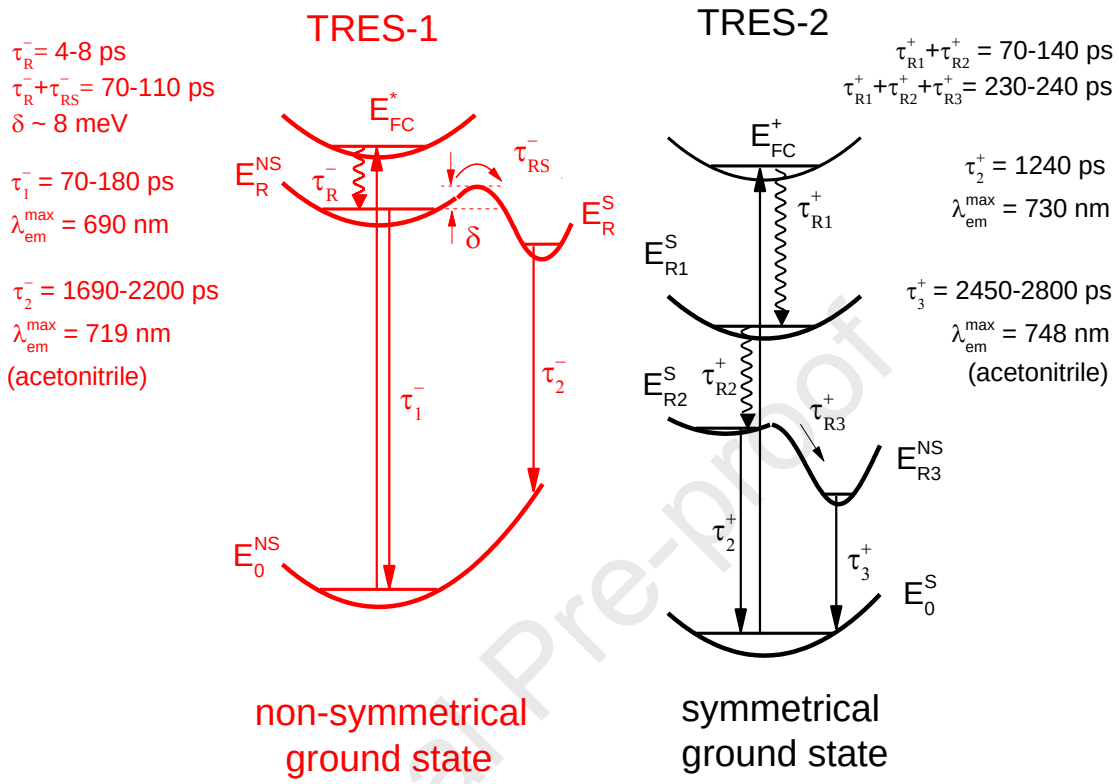

Fig. 8. Energy diagram for low-temperature relaxation paths of the excited states with different lifetimes. E^{NS}_0 is the non-symmetrical ground state, $E^*_{FC,}$ E^{NS}_R and E^S_R (in red) reflecting excited states of PC dye in the non-symmetrical ground state; E^S_0 is the symmetrical ground state, $E^+_{FC,}$ E^S_{R1}, E^S_{R2}, and E^{NS}_{R3} (in black) are excited states of PC dye in the symmetrical ground state.

During the lifetime of the excited state of the molecule, there is a symmetry breaking of the molecular geometry and establishing a non-symmetric excited state (E^{NS}_{R3}, Fig. 8). A similar effect was previously observed by our group in TRES studies of indocarbocyanine dye (astraphloxin) [15] and theoretically predicted by quantum-chemical analysis [16]. Such effect is observed in the TRES-2 group via the appearance of a new band at 748 nm at *t* = 29 ns (Fig. 5b). This band reflects the transition of an electron from the non-symmetric excited state

E^{NS}_{R3} to the ground state E^{S}_{0}. The average lifetime of the emission from E^{NS}_{R3} to E^{S}_{0} in the range of this band (τ^{+}_{3}) is approximately 2450-2800 ps (τ_2, τ_3 in Table 2). The transition time to the non-symmetric excited state (E^{NS}_{R3}) considering nonradiative processes of establishing electronic populations of bond and atom lengths, as well as establishing bond lengths corresponding to this non-symmetric excited state, is $\tau^{+}_{R1} + \tau^{+}_{R2} + \tau^{+}_{R3}$ = 230-240 ps (Fig. 8) featuring the $t_{1/2}$ for TRES-2.

For non-symmetric PC molecules in the ground state with predominant polyene structure (associated with the TRES-1 group), the PL emission is preceded by the absorption transition from the ground state (E^{NS}_{0}) to the excited FC state (E^{*}_{FC}) and then followed by nonradiative transition without symmetry breaking from FC excitonic state (E^{*}_{FC}) into the relaxed non-symmetric excitonic state (E^{NS}_{R}) by the time of τ^{-}_{R} =4-8 ps (Fig. 8). The PL band with a maximum of 690 nm (lifetime τ^{-}_{1} = 70-180 ps; τ_1, τ_2 in Table 2 for 710-720 nm) reflects the transition from E^{NS}_{R} to E^{NS}_{0} level. Along with the radiative transition from the E^{NS}_{R} state (690 nm band), a nonradiative transition to the E^{S}_{R} state with symmetric charge arrangement occurs (having a small barrier δ to overcome). The nonradiative processes of molecular relaxation to the radiative state (E^{S}_{R}) occur with the relaxation time of $\tau^{-}_{R} + \tau^{-}_{RS}$ = 70-110 ps characterized by $t_{1/2}$ for TRES-1. The PL band with a maximum at 719 nm can be associated with the radiative transition from the E^{S}_{R} state to the ground state with τ^{-}_{2} = 1690-2200 ps (τ_3 in Table 2).

The proposed diagram can be characteristic for cationic cyanines of polymethine and polyene nature, where excess charge has various distributions at the carbon chain between the TGs [1-3,15,19]. In future, carbon chain length dependence of electronic relaxation pathways needs to be studied to give more comprehensive picture of charge symmetry perturbations in carbon chains. In general, the model provides valuable insight for the relaxation processes depending on the charge localization for carbon chain based oligomers and polymers [9-

12,38,39], single-walled carbon nanotubes [18,42,43] or monatomic linear carbon chains (e.g. oligoynes, polyynes, cumulenes) [44,45]. The extent and contribution of charge localization need to be considered for such carbon-based systems to advance its potential applications in the area of nano-electronics and photonics.

4. SUMMARY

Thus, combined quantum-chemical calculations and time-resolved spectral measurements have allowed us to study the nature and the relaxation paths of the optically excited state of the cationic PC dye. The PL spectra for the dye were studied with picosecond time resolution, and two types of PL radiation were discriminated, which can be associated with the charge state of the carbon chain and symmetry breaking in the ground state. One group of PL spectra (TRES-1) featured by the peaks of 690 and 719 nm with delay times $t_{1/2}$ = 70-110 ps is characterizing the predominant non-symmetrical structure of the molecule in the ground state. Additionally, a short-wavelength shift of the transient absorption peaks in the range of 690-720 nm and a delay of 100-150 ps characterize the formation of small radius polarons in the chain of the molecule. Upon optical excitation of the molecule, a molecular exciton forms and quickly auto-localizes, and such auto-localized exciton can interact with an excess charge and form bound charged exciton states, which could be associated with induced absorption peaks observed in the pump-probe experiments.

The second PL group (TRES-2) having strong emission in the spectral region of λ_{EM} = 720-750 nm with $t_{1/2}$ = 230-240 ps is attributed to the symmetrical form of the molecule in the ground state. For the symmetrical form, the excess charge is delocalized on the carbon chain in the form of a large radius polaron, which defines the conformational and electronic structure of the carbon chain. According to the transient absorption spectra, the bond lengths

in the carbon chain of the dye molecule equalize during 40-100 ps, which is attributed to the formation of large radius polarons.

REFERENCES

1. Bach G, Daehne S. Cyanine dyes and related compounds, in ROOD'S Chemistry of Carbon Compounds, 2nd suppl. to 2nd ed., Vol. IVB, Het. Comp., Sainsbury M., Ed., Ch. 15. Amsterdam: Elsevier Science; 1997, p. 383-481.
2. Mishra A, Behera RK, Behera PK, Mishra BK, Behera GB. Cyanines during the 1990s: A review. Chem Rev 2000;100:1973-2011.
3. Bricks JL, Kachkovskii AD, Slominskii YL, Gerasov AO, Popov SV. Molecular design of near infrared polymethine dyes: A review. Dyes Pigm 2015;121:238-255.
4. Terenziani F, Przhonska OV, Webster S, Padilha LA, Slominsky YL, Davydenko IG, Gerasov AO, Kovtun YP, Shandura MP, Kachkovski AD. et al. Essential-state model for polymethine dyes: Symmetry breaking and optical spectra. J Phys Chem Lett 2010;1(12):1800-1804.
5. Pugh D. Exitons in the polyenes. Mol Phys 1973;26:1297-1310.
6. Davidov AS, Kislukha NI. Deformatsiya polienovykh molekul pri elektronnom vozbuzhdenii. Ukr J Phys 1973;19:672-679. (In Russian)
7. Kislukha NI, Karbovskii AV, Matveychuk SG. Spektry pogloshcheniya i izlucheniya korotkikh polienovykh tsepochek nakhodyashchikhsa v tverdykh rastvoritelyakh. Preprint ИТФ-84-192P, ITP NASU: Kyiv, 1986, 19. (In Russian)
8. Wei X, Vardeny ZV, Sariciftci NS, Heeger AJ. Absorption-detected magnetic-resonance studies of photoexcitations in conjugated-polymer/C60 composites. Phys Rev B 1996;53, 2187.

9. Bredas JL, Street GB. Polarons, bipolarons, and solitons in conducting polymers. Acc Chem Res 1985;18(10):309-315.

10. Tolbert LM. Solitons in a box: the organic chemistry of electrically conducting polyenes. Acc Chem Res 1992;25:561-568.

11. Craw JS, Reimers JR, Bacskay GB, Wong AT, Hush NS. Soliton in finite- and infinite-length negative-defect trans-polyacetylene and the corresponding brooker (polymethinecyanine) cations. I. Geometry. Chem Phys 1992;167:77-99.

12. Craw JS, Reimers JR, Bacskay GB, Wong AT, Hush NS. Soliton in finite- and infinite-length negative-defect trans-polyacetylene and the corresponding brooker (polymethinecyanine) cations. II. Charge density wave. Chem Phys 1992;167:101-109.

13. Kachkovskii AD. The solitonic nature of the electronic structure of the ions of linear conjugated systems. Theor Exp Chem 2005;41(3):139-164.

14. Vasylyuk SV, Yashchuk VM, Viniychuk OO, Piryatinski YP, Sevryukova MM, Gerasov AO, Zyabrev KV, Kovtun YP, Shandura MP, Kachkovsky OD. The investigation of relaxation paths in dioxaborine anionic polymethine dyes detected by low-temperature time-resolved fluorescence. Mol Cryst Liq Cryst 2011;535:123-131.

15. Lutsyk P, Piryatinski Y, Kachkovsky O, Verbitsky A, Rozhin A. Unsymmetrical relaxation paths of the excited states in cyanine dyes detected by time-resolved fluorescence: Polymethinic and polyenic forms. J Phys Chem A 2017;121:8236-8246.

16. Sanchez-Galvez A, Hunt P, Robb MA, Olivucci M, Vreven T, Schlegel HB. Ultrafast radiationless deactivation of organic dyes: Evidence for a two-state two-mode pathway in polymethine cyanines. J Am Chem Soc 2000;122:2911-2924.

17. Lutsyk P, Piryatinski Y, AlAraimi M, Arif R, Shandura M, Kachkovsky O, Verbitsky A, Rozhin A. Emergence of additional visible range photoluminescence due to

aggregation of cyanine dye - astraphloxin on carbon nanotubes dispersed with anionic surfactant. J Phys Chem C 2016;120:20378-20386.

18. Marchenko S. Stability of trionic states in zigzag carbon nanotubes. Ukr J Phys 2012;57(10):1055-1059.

19. Ishchenko AA. Structure and spectral-luminescent properties of polymethine dyes. Russ Chem Rev 1991;60:865-884.

20. Piryatinski YP, Verbitsky AB, Lutsyk PM, Rozhin AG, Kachkovskii OD, Prostota YO, Brovarets VS, Kurdyukov VV. Suppression of Kasha's rule in higher excited states of 4-pyrilocyanines. Mol Cryst Liq Cryst 2018;672:33-40.

21. Ovchinnikov AA, Ukrainskii II, Kventsel' GV. Theory of one-dimensional Mott semiconductors and the electronic structure of long molecules having conjugated bonds, Sov Phys Usp 1973;15:575-591.

22. Davydov AS. Biology & quantum mechanics. US: Pergamon Press; 1982.

23. Kachkovski AD, Tolmachev AI, Slominski YL, Kudinova MA, Derevyanko NA, Zhukova OO. Electronic properties of polymethine systems 7: Soliton symmetry breaking and spectral features of dyes with a long polymethine chain. Dyes Pigm 2005;64:207-216.

24. Davydov AS. Solitons in quasi-one-dimensional molecular structures. Sov Phys Usp 1982;25:898–918.

25. Lackowicz JR. Principles of fluorescence spectroscopy. 3rd edition. US: Springer; 2006.

26. Bhattacharya B, Jana B, Bose D, Chattopadhyay N. Multiple emissions of benzil at room temperature and 77 K and their assignments from ab initio quantum chemical calculations. J Chem Phys 2011;134:044535.

27. Karpicz R, Ostapenko N, Ostapenko Y, Polupan Y, Lazarev I, Galunov N, Macernis M, Abramavicius D, Valkunas L. Unusual temperature dependence of the fluorescence decay in heterostructured stilbene. Phys Chem Chem Phys 2021;23:3447-3454.

28. Kudinova MA, Kachkovski AD, Kurdyukov VV, Tolmachev AI. Nature of the absorption bands of pyrylocyanines. 2. Influence of t-Bu, Ph and Th ring substituents. Dyes Pigm 2000;45:1-7.

29. Blonskyi V, Brodin MS, Shpak AP. Wide-band laser femtosecond complex and its potential for scientific research. Ukr J Phys Reviews 2006;3(2):93-125.

30. Shynkarenko Y, Dmytruk A, Dmitruk I, Blonskyi I, Korenyuk P, Sönnichsen C, Kotko A. Transient absorption of gold nanorods induced by femtosecond laser irradiation. Ukr J Phys 2014;59(3):331-335.

31. Frisch MJ, Trucks GW, Schlegel HB, Scuseria GE, Robb MA, Cheeseman JR, Montgomery Jr JA, Vreven T, Kudin KN, Burant JC, et al. GAUSSIAN03 Revision B.05, Pittsburgh, PA, 2003.

32. Fabian J. TDDFT-calculations of Vis/NIR absorbing compounds. Dyes Pigm 2010;84:36-53.

33. Jacquemin D, Zhao Y, Valero R, Adamo C, Ciofini I, Truhlar DG, Verdict: Time-dependent density functional theory "not guilty" of large errors for cyanines. J Chem Theory Comput 2012;8:1255-1259.

34. Eskandari M, Roldao JC, Cerezo J, Milián-Medina B, Gierschner J. Counterion-mediated crossing of the cyanine limit in crystals and fluid solution: Bond length alternation and spectral broadening unveiled by quantum chemistry. J Am Chem Soc 2020;142:2835−2843.

35. Suponitsky KYu, Timofeeva TV, Antipin MY, Molecular and crystal design of nonlinear optical organic materials. Russ Chem Rev 2006;75(6):457-496.

36. Yaltychenko OV, Kanarovsky EY, Perenos elektrona v molekulyarnom komplekse tipa donor-polimer-aktseptor. Elektronnaya Obrabotka Materialov 2008;6:63-65. (In Russian).

37. Eggins BR. Khimicheskaya struktura i reaktsyonnaya sposobnost' tverdykh veschchestv. Moscow: Khimiya; 1976, p. 109-120. (In Russian)

38. Salaneck WR, Friend RH, Bredas JL. Electronic structure of conjugated polymers: consequences of electron-lattice coupling. Phys Rep 1999;319:231-251.

39. Agrinskaya NV. Molekulyarnaya elektronika. St.-Petersburg: SPbGPU; 2004 (in Russian)

40. Bai Y, Olivier J, Bullard G, Liu C, Therien MJ. Dynamics of charged excitons in electronically and morphologically homogeneous single-walled carbon nanotubes. PNAS 2018;115(4):674-679.

41. Cresi JSP, Di Mario L, Catone D, Martelli F, Paladini A, Turchini S, D'Addato S, Luches P, O'Keeffe P. Ultrafast Formation of Small Polarons and the Optical Gap in CeO2. J Phys Chem Lett 2020;11(14);5686-5691.

42. Mistakidis SI, Katsimiga GC, Koutentakis GM, Busch Th, Schmelcher P. Pump-probe spectroscopy of Bose polarons: Dynamical formation and coherence. Phys Rev Research 2020;2:033380.

43. Lutsyk P, Piryatinski Y, Shandura M, AlAraimi M, Tesa M, Arnaoutakis GE, Melvin AA, Kachkovsky O, Verbitsky A, Rozhin A. Self-assembly for two types of

j-aggregates: cis-isomers of dye on the carbon nanotube surface and free aggregates of dye trans-isomers. J Phys Chem C 2019;123(32):19903–19911.

44. Kutrovskaya S, Osipov A, Baryshev S, Zasedatelev A, Samyshkin V, Demirchyan S, Pulci O, Grassano D, Gontrani L, Hartmann RR, Portnoi ME, Kucherik A, Lagoudakis PG, Kavokin A. Excitonic fine structure in emission of linear carbon chains. Nano Lett 2020;20(9):6502-6509.

45. Bryce MR. A review of functional linear carbon chains (oligoynes, polyynes, cumulenes) and their applications as molecular wires in molecular electronics and optoelectronics. J Mater Chem C 2021; DOI: 10.1039/d1tc01406d

Highlights

- Pathways of excitation relaxation at low temperature in cationic dye are studied.
- Symmetric and non-symmetric localization of cationic charge in the dye is possible.
- Quantum-chemical calculations and time-resolved spectral measurements were used.
- Polymethine structure of the dye is attributed to large-radius polaron formation.
- The exciton model is applied for polyene structures of the dye.

Declaration of interests

☒ The authors declare that they have no known competing financial interests or personal relationships that could have appeared to influence the work reported in this paper.

☐The authors declare the following financial interests/personal relationships which may be considered as potential competing interests: